

# Structure refinements of $\text{Na}_{0.8}\text{Ti}_{1.2}\text{Ga}_{4.8}\text{O}_{10}$ : X-ray diffraction analysis for the sodium ion distribution in a one-dimensional tunnel-like space

Yuichi Michiue\* and Akira Sato

Advanced Materials Laboratory, National Institute for Materials Science, 1-1 Namiki, Tsukuba, Ibaraki 305-0044, Japan

Correspondence e-mail:  
michiue.yuichi@nims.go.jp

Received 1 June 2004

Accepted 20 September 2004

The structure of  $\text{Na}_{0.8}\text{Ti}_{1.2}\text{Ga}_{4.8}\text{O}_{10}$  was determined by means of single-crystal X-ray diffraction at 173 and 123 K and reinvestigated at 299 K. The host structure containing one-dimensional tunnels was retained over the temperatures examined, while significant changes were observed in the probability density distribution of  $\text{Na}^+$  ions in the tunnel. The refinement based on the local structure model with the deviated  $\text{Na}^+$  ion neighboring the vacancy gave a similar result to that from the conventional model, but with reduced standard uncertainties of the structural parameters for the  $\text{Na}^+$  ions. The potential barrier for the  $\text{Na}^+$  ion hopping between adjacent cavities was estimated to be *ca* 30–40 meV from the joint probability density function of deviated  $\text{Na}^+$  ions.

## 1. Introduction

There are some structures with one-dimensional tunnels of a large cross section, which are used for the ion-conduction path (Bernasconi *et al.*, 1979) or the immobilization of radioactive wastes (Ringwood *et al.*, 1979). Sodium titanogallate,  $\text{Na}_{0.8}\text{Ti}_{1.2}\text{Ga}_{4.8}\text{O}_{10}$ , is one of these compounds containing  $\text{Na}^+$  ions in a one-dimensional tunnel with an octagonal cross section (Michiue & Watanabe, 1994). The AC impedance measurement of  $\text{Na}_{0.8}\text{Ti}_{1.2}\text{Ga}_{4.8}\text{O}_{10}$  clarified the complicated frequency dependence that is often seen in one-dimensional tunnel structures, although a distinct frequency-independent conductivity was not observed between 293 and 193 K (Michiue, Y. & Yoshikado, S., unpublished). It was also reported that  $\text{Na}^+$  ions in this compound are exchanged for Li ions by keeping the sample in molten  $\text{LiNO}_3$  at 713 K (Michiue *et al.*, 1995). The coordination environment of the Li ion, which was definitely different from that of the  $\text{Na}^+$  ion, was clarified by neutron diffraction analysis (Michiue *et al.*, 1998). Ion exchange is usually observed in materials with layered structures or three-dimensional tunnel structures. It is, however, rare that the one-dimensional tunnel is used for the ion-exchange path.

In the structure of  $\text{Na}_{0.8}\text{Ti}_{1.2}\text{Ga}_{4.8}\text{O}_{10}$  (Fig. 1) the one-dimensional tunnel, which is a linear connection of distorted octahedral cavities formed by six O ions, is extended along **b**.  $\text{Na}^+$  ions are located in these cavities. The compound is generally expressed by  $\text{Na}_x\text{Ti}_{2-x}\text{Ga}_{4+x}\text{O}_{10}$  ( $0 \leq x \leq 1$ ) and the Na density per cavity is given by *x*. Namely, 80% of the cavities are occupied by  $\text{Na}^+$  ions and the rest are vacant in  $\text{Na}_{0.8}\text{Ti}_{1.2}\text{Ga}_{4.8}\text{O}_{10}$ . It was concluded from the previous study (Michiue & Watanabe, 1994) that significant deviating along **b** is observed for part of the  $\text{Na}^+$  ions and the structure is best described by distributing  $\text{Na}^+$  ions at two sites, Na1 (0, 0, 0.5) and Na2 [0, 0.28 (6), 0.5]. The two Na sites are so close that

structural parameters for the  $\text{Na}^+$  ions suffer a strong correlation to each other and have large estimated standard uncertainties (s.u.s). The atomic displacement parameters (ADPs) of  $\text{Na}^+$  ions were very large, as is often observed for guest ions in tunnel-like host structures. The partially disordered character of ions with pronounced displacements in cavities is of interest from the viewpoint of material chemistry or physics, but troublesome in structural characterization. In order to investigate the nature of guest ions in this kind of material, it is helpful to clarify the structural parameters over a wide range of temperatures. It is expected that difficulties in the refinement are reduced at low temperature because of less thermal motion for guest ions. In this study, single-crystal X-ray diffraction intensities were measured at 173 and 123 K, as well as at room temperature for reinvestigation. Refinements were carried out using several models with different constraints, and probability density functions (PDFs) were drawn from the structural parameters obtained. The PDF analysis is useful in investigating ions with large displacements and the one-particle potential (OPP) is available from the joint-PDF (Bachmann & Schulz, 1984).

## 2. Experimental

Single crystals of  $\text{Na}_{0.8}\text{Ti}_{1.2}\text{Ga}_{4.8}\text{O}_{10}$  were obtained by the slow cooling method. A mixture of 0.283 g of  $\text{Na}_2\text{CO}_3$ , 0.639 g of  $\text{TiO}_2$  and 0.999 g of  $\text{Ga}_2\text{O}_3$  ( $\text{Na}_2\text{CO}_3:\text{TiO}_2:\text{Ga}_2\text{O}_3 = 1:2:3$  as a molar ratio) was heated with 7.997 g of the  $\text{Na}_2\text{CO}_3\text{-MoO}_3$  flux (3.392 g of  $\text{Na}_2\text{CO}_3$  and 4.605 g of  $\text{MoO}_3$  or

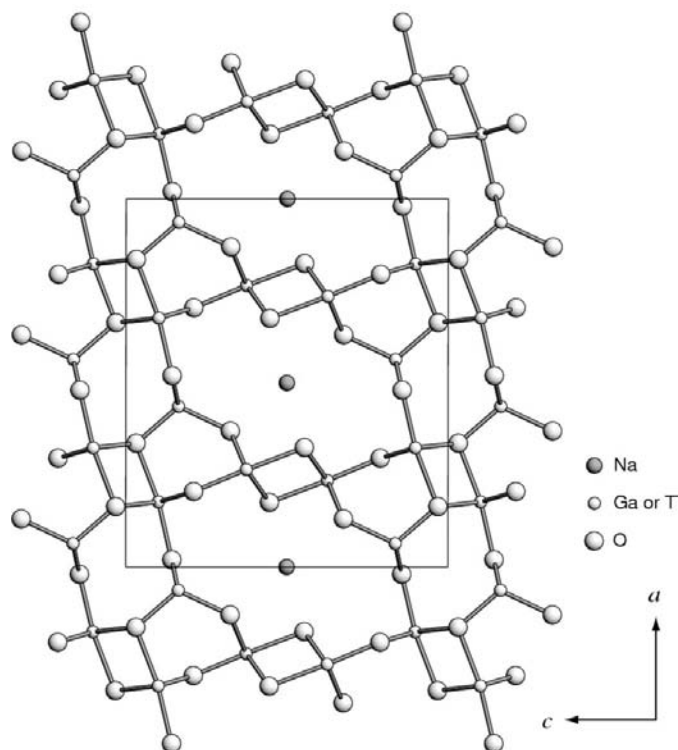


**Figure 1**  
Structure of  $\text{Na}_{0.8}\text{Ti}_{1.2}\text{Ga}_{4.8}\text{O}_{10}$  projected along **b**.

$\text{Na}_2\text{CO}_3:\text{MoO}_3 = 1:1$  as a molar ratio) at 1573 K for 10 h. The sample was cooled to 1473 K at a rate of  $4\text{ K h}^{-1}$  and then taken out of the furnace. The flux was dissolved in water to separate needle-shaped crystals of  $\text{Na}_{0.8}\text{Ti}_{1.2}\text{Ga}_{4.8}\text{O}_{10}$ .

Conditions and parameters for data collection and refinement are listed in Table 1.<sup>1</sup> An analytical absorption correction was applied for a crystal bounded by  $\{1\ 0\ 0\}$  at a distance of 0.08 mm from the crystal center,  $\{0\ 1\ 0\}$  at 0.12 mm and  $\{0\ 0\ 1\}$  at 0.05 mm. No optimization for the dimensions was carried out. The  $\sigma(I_o)$  value for each independent reflection was calculated by two methods: one is based on the Poisson distribution and another using equivalents, and the larger one was taken. The one-atom model for Na (model I) and two types of split-atom models (model II and model III) were used for the refinements at all temperatures. Model I contains only one Na site, Na1, at the cavity center (0, 0, 0.5), while two Na sites, Na1 and Na2 (0, y, 0.5), were taken in the latter two models. In all the models, full occupation at the *M* site by Ga and Ti was assumed, that is  $a[\text{Ti}] = 0.5 - a[\text{Ga}]$ , where the  $a[A]$  is the number of *A* ions in a unit cell divided by the site multiplicity of a general position, 8. (The conventional site occupancy  $\text{occ}[A]$  in Table 2 is given by  $\text{occ}[A] = 8a[A]/m[A]$ , where  $m[A]$  is the site multiplicity of the *A* site.) The charge neutrality of the whole crystal was also assumed for all models. Namely,  $a[\text{Na}1] = a[\text{Ga}]$  for model I and  $a[\text{Na}2] = a[\text{Ga}] - a[\text{Na}1]$  for model II. In model III an additional condition was imposed so that the number of  $\text{Na}^{2+}$  ions was twice the number of vacancies, which was deduced from the local structure model for the Na arrangement shown in Fig. 2. (Detailed explanations for the model are given in §3.) Thus, the constraints in model III were  $a[\text{Ti}] = 0.5 - a[\text{Ga}]$ ,  $a[\text{Na}1] = 3a[\text{Ga}] - 0.5$  and  $a[\text{Na}2] = 0.5 - 2a[\text{Ga}]$ , with the standard uncertainties (s.u.s) of the refined parameters for  $\text{Na}^+$  ions being effectively reduced compared with those from model II. In model I, fourth-order Gram–Charlier terms (Johnson & Levy, 1974; Kuhs, 1992) were introduced for the atomic displacement of Na1. The harmonic terms of Na1 were fixed in refinements with anharmonic ADPs at all the temperatures; otherwise refinements gave unrealistically deformed PDFs with considerable negative regions. The anharmonic atomic displacement was also tested for split-atom models, in which third-order terms for Na2 were applied with no anharmonic terms for Na1. However, the s.u.s of refined parameters were almost comparable to or larger than the parameters themselves, and no significant improvement was detected in the reliability factors. Results from model III with harmonic ADPs were taken as final and are summarized in Table 1. PDF, joint-PDF and OPP for the  $\text{Na}^+$  ion were drawn from obtained structural parameters. All calculations were performed using the program package *JANA2000* (Petricek & Dusek, 2000).

<sup>1</sup> Lists of observed and calculated structure factors, final structural parameters, selected interatomic distances from the model III, structural parameters with anharmonic ADPs used for drawing the potential curve, and residual density maps at the section  $x = 0.5$  for the model I with anharmonic ADPs and the model III with harmonic ADPs have been deposited. Supplementary data for this paper are available from the IUCr electronic archives (Reference: LC5009). Services for accessing these data are described at the back of the journal.

**Table 1**  
Experimental details.

	299 K model III	173 K model III	123 K model III
<b>Crystal data</b>			
Chemical formula	Ga <sub>4.8</sub> Na <sub>0.8</sub> O <sub>10</sub> Ti <sub>1.2</sub>	Ga <sub>4.8</sub> Na <sub>0.8</sub> O <sub>10</sub> Ti <sub>1.2</sub>	Ga <sub>4.8</sub> Na <sub>0.8</sub> O <sub>10</sub> Ti <sub>1.2</sub>
$M_r$	570.5	570.5	570.5
Cell setting, space group	Monoclinic, <i>C2/m</i>	Monoclinic, <i>C2/m</i>	Monoclinic, <i>C2/m</i>
$a, b, c$ (Å)	12.1008 (8), 3.0113 (2), 10.4100 (6)	12.0848 (12), 3.0101 (3), 10.4014 (9)	12.0828 (9), 3.0099 (3), 10.4045 (7)
$\beta$ (°)	92.258 (4)	92.187 (5)	92.192 (4)
$V$ (Å <sup>3</sup> )	379.04 (4)	378.09 (6)	378.11 (5)
$Z$	2	2	2
$D_x$ (Mg m <sup>-3</sup> )	4.997 (1)	5.010 (1)	5.009 (1)
Radiation type	Mo $K\alpha$	Mo $K\alpha$	Mo $K\alpha$
No. of reflections for cell parameters	967	854	871
$\theta$ range (°)	3.8–51.6	3.8–51.4	3.9–51.4
$\mu$ (mm <sup>-1</sup> )	18.11	18.16	18.16
Temperature (K)	299	173	123
Crystal form, color	Prism, colorless	Prism, colorless	Prism, colorless
Crystal size (mm)	0.24 × 0.16 × 0.10	0.24 × 0.16 × 0.10	0.24 × 0.16 × 0.10
<b>Data collection</b>			
Diffractometer	Bruker SMART APEX CCD area detector	Bruker SMART APEX CCD area detector	Bruker SMART APEX CCD area detector
Data collection method	$\omega$ scans	$\omega$ scans	$\omega$ scans
Absorption correction	Analytical	Analytical	Analytical
$T_{\min}$	0.074	0.071	0.073
$T_{\max}$	0.249	0.250	0.250
No. of measured, independent and observed reflections	5633, 2168, 1785	5581, 2159, 1749	5596, 2160, 1752
Criterion for observed reflections	$I > 2\sigma(I)$	$I > 2\sigma(I)$	$I > 2\sigma(I)$
$R_{\text{int}}$	0.060	0.060	0.059
$\theta_{\text{max}}$ (°)	51.7	51.6	51.7
Range of $h, k, l$	–24 ⇒ $h$ ⇒ 21 –6 ⇒ $k$ ⇒ 5 –22 ⇒ $l$ ⇒ 22	–24 ⇒ $h$ ⇒ 21 –6 ⇒ $k$ ⇒ 5 –22 ⇒ $l$ ⇒ 22	–24 ⇒ $h$ ⇒ 21 –6 ⇒ $k$ ⇒ 5 –22 ⇒ $l$ ⇒ 22
<b>Refinement</b>			
Refinement on	$F^2$	$F^2$	$F^2$
$R[F^2 > 2\sigma(F^2)], wR(F^2), S$	0.028, 0.069, 1.17	0.029, 0.067, 1.06	0.028, 0.065, 1.04
No. of reflections	2168	2159	2160
No. of parameters	60	60	60
Weighting scheme	Based on measured s.u.s; $w = 1/[\sigma^2(I) + 0.0004I^2]$	Based on measured s.u.s; $w = 1/[\sigma^2(I) + 0.0004I^2]$	Based on measured s.u.s; $w = 1/[\sigma^2(I) + 0.0004I^2]$
$(\Delta/\sigma)_{\text{max}}$	0.007	0.010	0.008
$\Delta\rho_{\text{max}}, \Delta\rho_{\text{min}}$ (e Å <sup>-3</sup> )	2.88, –1.95	3.10, –2.21	2.92, –1.99
Extinction method	B-C type 2 (Becker & Coppens, 1974)	B-C type 2 (Becker & Coppens, 1974)	B-C type 2 (Becker & Coppens, 1974)
Extinction coefficient	0.001741	0.002039	0.00195

Computer programs used: JANA2000 (Petricek & Dusek, 2000).

### 3. Results and discussion

The framework structure of Na<sub>0.8</sub>Ti<sub>1.2</sub>Ga<sub>4.8</sub>O<sub>10</sub> was essentially independent of temperature. Structural parameters concerning the Na<sup>+</sup> ions from the three models are listed in Table 2. Parameters in model II at room temperature were almost identical to those from the previous study (Michiue & Watanabe, 1994), in which the same constraints as in model II were used, despite the fact that the single crystals used in the two studies were taken from different batches. In model I with harmonic ADPs for all atoms, the reliability factors  $R_{\text{obs}}(F)/wR_{\text{obs}}(F^2)$  were 0.0284/0.0685 (299 K), 0.0299/0.0669 (173 K) and 0.0287/0.0648 (123 K), which were improved a little by applying anharmonic terms for Na1, as shown in Table 2. However, the s.u.s of the anharmonic terms were almost comparable to or larger than the parameters themselves. The final reliability factors are a little inferior to those by split-

atom models at all the temperatures, while the number of parameters was 60, 61 and 60 for model I with anharmonic ADPs, model II with harmonic ADPs and model III with harmonic ADPs, respectively. The maximum and minimum residuals in the tunnel (the volume with  $0.45 < x < 0.55$  and  $0.4 < z < 0.6$  is considered as in the tunnel for convenience) for model I with anharmonic ADPs, 1.20 and  $-1.14 \text{ e \AA}^{-3}$  at 299 K, 2.17 and  $-1.95 \text{ e \AA}^{-3}$  at 173 K, 1.65 and  $-1.72 \text{ e \AA}^{-3}$  at 123 K, were reduced to 0.83 and  $-1.14 \text{ e \AA}^{-3}$  at 299 K, 1.07 and  $-1.63 \text{ e \AA}^{-3}$  at 173 K, and 0.94 and  $-1.43 \text{ e \AA}^{-3}$  at 123 K for model III with harmonic ADPs. (Note that the minimum and the maximum densities given in Table 2 are not in the tunnel but near the framework metal ions.) Thus, the structure is better described by the split-atom model than by the one-atom with the anharmonic ADPs at room temperature and below. It was also reported for a hollandite with a one-dimensional tunnel structure that the higher the temperature,

**Table 2**  
Structural parameters for Na<sup>+</sup> ions and reliability factors in three structure models.

	Model I, anharmonic ADPs	Model II, harmonic ADPs	Model III, harmonic ADPs
299 K			
Na1 <sup>†</sup> Occupancy	0.800 (6)	0.59 (6)	0.421 (19)
$U^{22}$	0.292‡	0.13 (3)	0.081 (10)
$U_{eq}$	0.117‡	0.060 (9)	0.045 (4)
Na2 <sup>†</sup> Occupancy		0.11 (3)	0.193 (6)
$y$		0.30 (3)	0.225 (11)
$U^{22}$		0.09 (3)	0.16 (2)
$U_{eq}$		0.059 (13)	0.075 (9)
Na/cavity§	0.800 (6)	0.806 (6)	0.808 (6)
$R_{obs}(F)$ , $wR_{obs}(F^2)$	0.0280, 0.0677	0.0280, 0.0672	0.0280, 0.0672
$R_{all}(F)$ , $wR_{all}(F^2)$	0.0367, 0.0690	0.0367, 0.0685	0.0367, 0.0685
$S_{obs}$ , $S_{all}$	1.28, 1.18	1.27, 1.17	1.27, 1.17
173 K			
Na1 <sup>†</sup> Occupancy	0.808 (6)	0.26 (10)	0.433 (19)
$U^{22}$	0.281‡	0.035 (16)	0.064 (8)
$U_{eq}$	0.108‡	0.030 (7)	0.037 (3)
Na2 <sup>†</sup> Occupancy		0.28 (5)	0.189 (6)
$y$		0.17 (3)	0.223 (9)
$U^{22}$		0.15 (4)	0.108 (16)
$U_{eq}$		0.064 (12)	0.050 (6)
Na/cavity§	0.808 (6)	0.812 (6)	0.810 (6)
$R_{obs}(F)$ , $wR_{obs}(F^2)$	0.0296, 0.0662	0.0293, 0.0657	0.0293, 0.0658
$R_{all}(F)$ , $wR_{all}(F^2)$	0.0402, 0.0678	0.0399, 0.0673	0.0399, 0.0673
$S_{obs}$ , $S_{all}$	1.16, 1.07	1.16, 1.06	1.16, 1.06
123 K			
Na1 <sup>†</sup> Occupancy	0.802 (6)	0.34 (11)	0.410 (18)
$U^{22}$	0.274‡	0.034 (15)	0.045 (6)
$U_{eq}$	0.103‡	0.027 (6)	0.029 (2)
Na2 <sup>†</sup> Occupancy		0.23 (5)	0.197 (6)
$y$		0.20 (3)	0.217 (7)
$U^{22}$		0.11 (3)	0.086 (11)
$U_{eq}$		0.044 (11)	0.038 (4)
Na/cavity§	0.802 (6)	0.804 (6)	0.804 (6)
$R_{obs}(F)$ , $wR_{obs}(F^2)$	0.0285, 0.0642	0.0282, 0.0634	0.0282, 0.0634
$R_{all}(F)$ , $wR_{all}(F^2)$	0.0395, 0.0659	0.0392, 0.0651	0.0392, 0.0651
$S_{obs}$ , $S_{all}$	1.14, 1.05	1.13, 1.04	1.13, 1.04

<sup>†</sup> Fractional coordinates are (0, 0, 0.5) for Na1 and (0,  $y$ , 0.5) for Na2. <sup>‡</sup> Harmonic ADPs were fixed in the final refinement with fourth-order terms. <sup>§</sup> The total number of Na ions per cavity.

the better the one-atom model describes the structure (Weber & Schulz, 1986). At a stage with isotropic displacement parameters in model II, the occupancies at the two Na sites were almost independent of temperature. The occ[Na1]/occ[Na2] ratios were 0.412 (18)/0.199 (10), 0.415 (17)/0.201 (9) and 0.424 (14)/0.194 (8) at 299, 173 and 123 K, respectively. Fluctuations of the  $y$  fractional coordinates for Na2 were small at all the temperatures; 0.216 (4) (299 K), 0.211 (4) (173 K) and 0.214 (3) (123 K). By the application of anisotropic displacements, the total number of Na<sup>+</sup> ions per cavity was kept almost constant at all temperatures, as shown in Table 2. (Note that there are one Na1 and two Na2 sites in a cavity.) However, the occupation factors at the two Na sites changed appreciably with the accompanying position shift of Na2 at 299 and 173 K, while changes were within the s.u.s at 123 K. Strangely, this tendency was reversed between 299 and 173 K. It is likely that the two Na sites are close enough to cause strong correlations between the parameters of the two sites

and consequently large s.u.s. The correlation coefficient between the occupation factor at Na1 and the fractional coordinate  $y$  of Na2, for example, exceeded 0.9 at all temperatures.

It is commonly believed for one-dimensional tunnel structures that the deviation of guest ions is related to a vacancy (Beyeler, 1976). It is likely that an Na<sup>+</sup> ion suffers considerably from repulsive interactions from neighboring Na<sup>+</sup> ions because the distance between the neighboring cavity centers is only *ca* 3 Å, that is the cell dimension  $b$ . Therefore, if an Na<sup>+</sup> ion is located in a cavity with a vacant neighboring cavity, the ion deviates from the cavity center towards the vacant site to reduce the repulsion from an Na<sup>+</sup> ion in one of the other neighboring cavities, as schematically shown in Fig. 2. The Na1 site is reserved for Na<sup>+</sup> ions with both of the neighboring sites occupied and the Na2 site is for Na<sup>+</sup> ions with one of the neighboring sites occupied and the other site vacant. According to this model, the number of Na2<sup>+</sup> ions should be twice the number of vacancies, unless the Na density is so low as to allow two (or more) neighboring vacancies. However, occupancies at the Na1 and Na2 sites from model II deviated from values based on this expectation, especially at 299 and 173 K. Thus, in model III an additional constraint was imposed so as to realise the structure model in Fig. 2. Occupancies at two Na sites and the fractional coordinate  $y$  of the Na2 obtained in model III fluctuated less than those in model II, while reliability factors from the two split-atom models were identical. The PDF and the joint-PDF were drawn using the structural parameters obtained. The PDFs of the two Na sites overlap substantially even at 123 K, as shown in Fig. 3. The Na

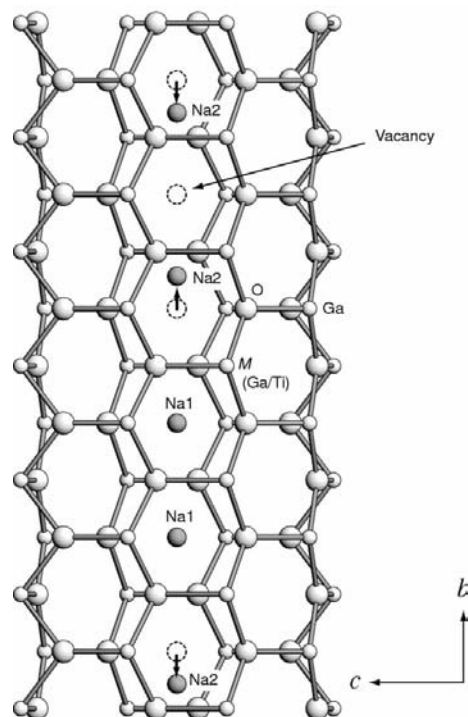


**Figure 2**  
Schematic representation of a postulated local arrangement of Na<sup>+</sup> ions in the tunnel.

density distribution in a cavity along the tunnel direction  $\mathbf{b}$ , which is the integral of the joint-PDF with respect to  $x$  and  $z$ , as expressed by  $\rho(y) = \sum_n \text{occ}_n (2\pi U_n^{22})^{-1/2} \exp\{-b^2(y_n - y)^2 / 2U_n^{22}\}$ , varied according to temperature, as shown in Fig. 4. It should be noted that distributions from the two models are very close to each other, despite different structural parameters. Different sets of the individual Na density make up similar summations, as demonstrated for plots at 173 K (Fig. 5). In the following discussion we use the parameter set from model III rather than model II, because the former generally has smaller s.u.s and coincides with the microscopic picture given in Fig. 2.

From the viewpoint of ionic conduction or ion transport in solids, it is of significance to estimate the potential barrier which an  $\text{Na}^+$  ion experiences in the course of hopping from a site onto a neighboring one. An  $\text{Na}^+$  ion is obviously immobile unless at least one of the neighboring sites is vacant. Accordingly, the contribution of Na1 should be eliminated in the evaluation of the potential barrier in the ion-hopping process. The OPP along the tunnel direction  $\mathbf{b}$  was calculated between  $(0, 0, 0.5)$  and  $(0, 1, 0.5)$  from the joint-PDF of the mobile ion, Na2, in model III. The barrier height  $\Delta E_b$ , given by a potential value at  $(0, 0.5, 0.5)$ , was almost independent of temperature; 39, 38 and 37 meV at 299, 173 and 123 K, respectively. This is plausible because the activation energy is constant over a wide range of temperatures for most of the ion conductors, giving a straight line in the Arrhenius plot. It is further assumed that the potential energy for the  $\text{Na}^{2+}$  ion increases infinitely in the direction of the occupied neighboring site, because two  $\text{Na}^+$  ions cannot be accommodated in a cavity. On the other hand, the potential curve has its maximum in the direction of the vacant neighboring site, giving the finite potential barrier in the ion-hopping process. As the environment of the  $\text{Na}^{2+}$  ion is thus asymmetric in the  $y$  direction, it is suggested that the PDF of Na2 is asymmetrically deformed. Anharmonic ADPs were taken for Na2 in successive refinements for model III. Conventional refinement with

third-order Gram–Charlier terms was successful at 173 and 123 K, but harmonic terms were fixed to prevent the diverging of parameters in refinements at 299 K. The PDF was deformed by the introduction of third-order terms so as to increase the density at the bottlenecking point  $(0, 0.5, 0.5)$  at 173 K, which lowered the barrier height  $\Delta E_b$  to 31 meV, as shown in Fig. 6. The PDF at 123 K splits into two paths in the vicinity of  $y = 0.5$ , which is plausible because the deviation of the Na2 from the  $(0, y, 0.5)$  axis reduces the repulsive interaction from O4 ions at  $(0.1754, 0.5, 0.5543)$  and  $(-0.1754, 0.5, 0.4457)$ . The potential barrier along the curved path deviating from the  $(0, y, \frac{1}{2})$  axis was *ca* 34 meV. Thus, the barrier height in the Na hopping in this one-dimensional tunnel structure was estimated to be between 30 and 40 meV. It should be noted that similar values (30–50 meV) were reported for the bottlenecking barrier in potassium hollandite between 133 and 387 K (Weber & Schulz, 1986), which coincides well with an

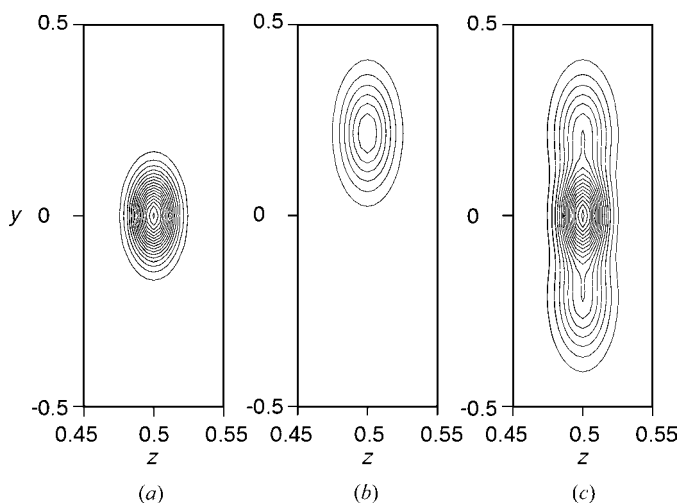


**Figure 3** PDF for (a) Na1, (b) Na2 and (c) the joint-PDF at  $x = 0$  and 123 K. The structural parameters used are from model III with the harmonic ADPs. Contour intervals are  $0.5 \text{ atom } \text{\AA}^{-3}$ .

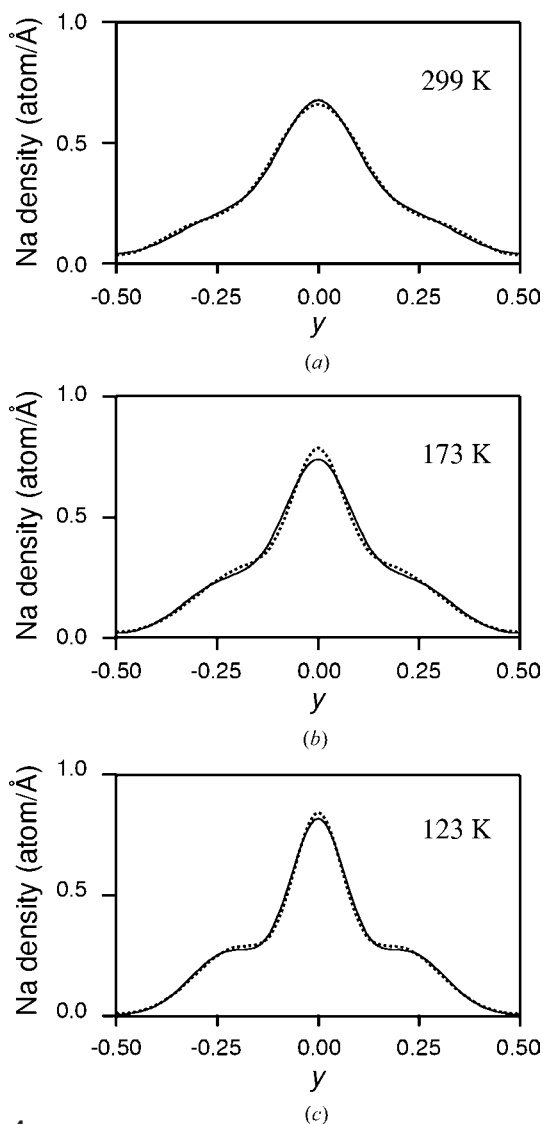


**Figure 4** Probability density distribution of the  $\text{Na}^+$  ion in a cavity along  $\mathbf{b}$  at (a) 299, (b) 173 and (c) 123 K from model II (dotted line) and model III (solid line) with harmonic ADPs. The joint-PDF was integrated with respect to  $x$  and  $z$  in the cavity.



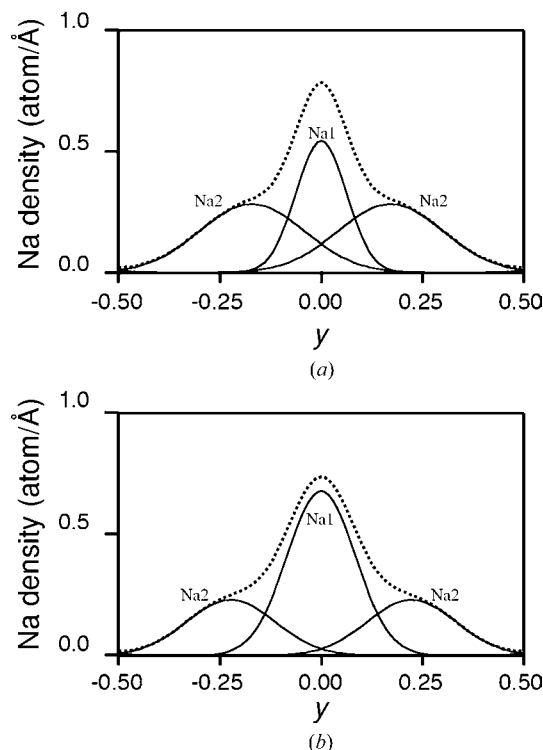


**Figure 5**  
Individual Na distributions from (a) model II and (b) model III with harmonic ADPs at 173 K.

activation energy of 34 meV (Khanna *et al.*, 1981) or 58 meV (Yoshikado *et al.*, 1982) from microwave measurements. Further discussion seems to be of little significance as the s.u.s of the refined parameters were almost comparable to the parameters themselves and no significant improvement was detected in the reliability factors compared with those with harmonic ADPs. Refinements with fourth-order terms for Na1 and/or Na2 gave unrealistic PDFs.

#### 4. Summary

In summary, the structure of  $\text{Na}_{0.8}\text{Ti}_{1.2}\text{Ga}_{4.8}\text{O}_{10}$  with a one-dimensional tunnel-like space containing  $\text{Na}^+$  ions was refined at 173 and 123 K, along with a reinvestigation at room temperature. The  $\text{Na}^+$ -ion distribution in the tunnel was well described by the split-atom model rather than the one-atom model with anharmonic ADPs at room and low temperatures. Split-atom refinements based on the local structure model with the deviated  $\text{Na}^+$  ion neighboring the vacancy (Fig. 2) gave a similar result to that from the conventional model with simple charge neutrality, but effectively reduced the s.u.s of

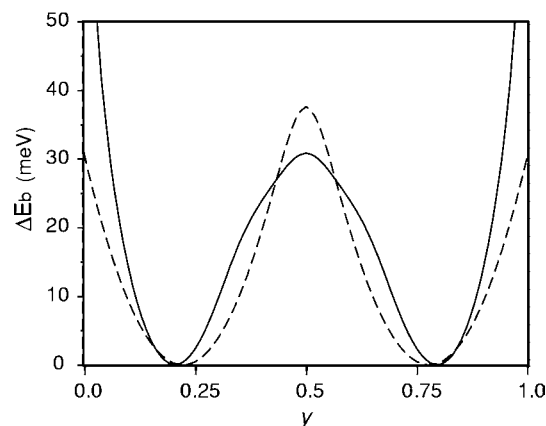


**Figure 6**  
Potential curves for Na2 between (0, 0, 0.5) and (0, 1, 0.5) in model III with anharmonic ADPs (solid line) and harmonic ADPs (broken line) at 173 K.

the structural parameters for  $\text{Na}^+$  ions. The potential barrier for the  $\text{Na}^+$  ion hopping between adjacent cavities was estimated to be *ca* 35–40 meV by the split-atom model with harmonic ADPs. The lower value of *ca* 30–35 meV was suggested by the introduction of anharmonic terms for the atomic displacement.

#### References

- Bachmann, R. & Schulz, H. (1984). *Acta Cryst.* **A40**, 668–675.  
 Becker, P. J. & Coppens, P. (1974). *Acta Cryst.* **A30**, 129–147.  
 Bernasconi, J., Beyeler, H. U. & Strassler, S. (1979). *Phys. Rev. Lett.* **42**, 819–822.  
 Beyeler, H. U. (1976). *Phys. Rev. Lett.* **37**, 1557–1560.  
 Johnson, C. K & Levy, H. A. (1974). *International Tables for X-ray Crystallography*, Vol. IV, pp. 311–336. Birmingham: Kynoch Press. (Present distributor Kluwer Academic Publishers, Dordrecht.)  
 Khanna, S. K., Gruner, G., Orbach, R. & Beyeler, H. U. (1981). *Phys. Rev. Lett.* **47**, 255–257.  
 Kuhs, W. F. (1992). *Acta Cryst.* **A48**, 80–98.  
 Michiue, Y., Takenouchi, S., Sasaki, T. & Watanabe, M. (1995). *Chem. Lett.* pp. 1105–1106.  
 Michiue, Y., Takenouchi, S., Sasaki, T., Watanabe, M., Izumi, F., Morii, Y. & Shimojo, Y. (1998). *Solid State Ion.* **113–115**, 471–475.  
 Michiue, Y. & Watanabe, M. (1994). *Solid State Ion.* **70/71**, 186–190.  
 Petricek, V. & Dusek, M. (2000). *JANA2000*. Institute of Physics, Praha, Czech Republic.  
 Ringwood, A. E., Kessen, S. E., Ware, N. G., Hibberson, W. & Major, A. (1979). *Nature*, **278**, 219–223.  
 Weber, H.-P. & Schulz, H. (1986). *J. Chem. Phys.* **85**, 475–484.  
 Yoshikado, S., Ohachi, T., Taniguchi, I., Onoda, Y., Watanabe, M. & Fujiki, Y. (1982). *Solid State Ion.* **7**, 335–344.